Available online at www.sciencedirect.com
SCIENCE DIRECT®
Chemistry and Physics of Lipids 132 (2004) 89–100
CPL
CHEMISTRY AND PHYSICS OF LIPIDS
www.elsevier.com/locate/chemphyslip

Solid-state nuclear magnetic resonance studies of HIV and influenza fusion peptide orientations in membrane bilayers using stacked glass plate samples

Christopher M. Wasniewski, Paul D. Parkanzky, Michele L. Bodner, David P. Weliky*

Departments of Chemistry and Physics, Michigan State University, East Lansing, MI 48824-1322, USA

Available online 12 October 2004

Abstract

The human immunodeficiency virus (HIV) and influenza virus fusion peptides are ~20-residue sequences which catalyze the fusion of viral and host cell membranes. The orientations of these peptides in lipid bilayers have been probed with ^{15}N solid-state nuclear magnetic resonance (NMR) spectroscopy of samples containing membranes oriented between stacked glass plates. Each of the peptides adopts at least two distinct conformations in membranes (predominantly helical or beta strand) and the conformational distribution is determined in part by the membrane headgroup and cholesterol composition. In the helical conformation, the ^{15}N spectra suggest that the influenza peptide adopts an orientation approximately parallel to the membrane surface while the HIV peptide adopts an orientation closer to the membrane bilayer normal. For the beta strand conformation, there appears to be a broader peptide orientational distribution. Overall, the data suggest that the solid-state NMR experiments can test models which correlate peptide orientation with their fusogenic function.

Keywords: Fusion; Peptide; HIV; Influenza; NMR; Membrane

1. Introduction

Enveloped viruses such as human immunodeficiency virus (HIV) and influenza are surrounded by a membrane which the viruses obtain during budding from a host cell. Infection of a new cell requires fusion of the viral and target cell membranes so that at the end of the fusion process, the viral nucleocapsid is inside the host cell and can initiate viral replication. HIV and influenza viral infection differ in that HIV fuses directly with the plasma membrane while influenza is first endocytosed and intracellular fusion occurs between the viral and endosomal membranes (Hernandez et al., 1996; Eckert and Kim, 2001). Although the membrane free energies are comparable before and after fusion, the fusion process is typically slow in cellular or model liposome systems in the absence of a catalyst. For viral/host cell fusion, the fusion rate is accelerated by proteins in the viral envelope membrane which carry out at least two important functions: (1)

* Corresponding author. Tel.: +1 517 355 9715x281; fax: +1 517 353 1793.
E-mail address: weliky@chemistry.msu.edu (D.P. Weliky).

0009-3084/$ – see front matter © 2004 Elsevier Ireland Ltd. All rights reserved.
doi:10.1016/j.chemphyslip.2004.09.008

targeting appropriate host cells by binding to specific host cell proteins; and (2) catalyzing membrane fusion through interactions with the cellular membrane and also possibly the viral membrane (Blumenthal et al., 2003). The ∼20-residue apolar 'fusion peptide' (FP) domains of these proteins play an important role in these catalytic interactions with membranes (Durell et al., 1997; Epand, 2003). The sequence of the FP differs between the HIV and influenza viruses but both viral FPs share a common topological feature of being at the N-terminus of an envelope protein, either gp41 (HIV) or the HA2 subunit of the hemagglutinin protein (influenza). FPs are sequestered in the envelope proteins prior to fusion, and the envelope protein conformational changes during the fusion process expose the FPs and allow them to interact with target membranes (Wilson et al., 1981; Carr and Kim, 1993; Bullough et al., 1994). For HIV, these conformational changes are triggered by envelope protein/host cell protein binding, while for influenza, they are triggered by the lowering of the pH to ∼5 in the endosome.

The main experimental evidence for the functional significance of the FPs is: (1) FP point mutations can render the virus fusion-inactive (Gething et al., 1986; Freed et al., 1992; Delahunty et al., 1996); (2) for influenza virus, the FPs are membrane-bound after fusion has occurred (Durrer et al., 1996); and (3) peptides composed of either the HIV FP (HFP) or influenza FP (IFP) sequences can induce mixing of lipids between large unilamellar vesicles (LUVs) or between red blood cells and the mutation-fusion activity relationships for the peptide-induced lipid mixing correlate with those of the viral/cell fusion (Durell et al., 1997; Pereira et al., 1997; Pritsker et al., 1999; Epand et al., 2001).

The present paper focuses on the model peptide systems. The previously described functional results suggest that these systems can provide relevant information about at least the lipid mixing step of membrane fusion (which occurs early in the fusion process). The biophysical literature and results in this paper show that both the HIV and influenza FPs can adopt at least two conformations in membranes, one predominantly helical and the other beta strand (Rafalski et al., 1990; Gordon et al., 1992; Martin et al., 1996; Durell et al., 1997; Curtain et al., 1999; Han and Tamm, 2000b; Yang et al., 2001a, 2002; Saez-Cirion and Nieva, 2002; Bodner et al., 2004). Literature models for the helical structures have been based in part on nuclear magnetic resonance (NMR) structures of the monomer FPs in detergent micelles (Chang et al., 1997; Dubovskii et al., 2000; Han et al., 2001; Hsu et al., 2002). The IFP in either sodium dodecylsulfate (SDS) or dodecylphosphocholine (DPC) detergent has an N-terminal helix of ∼11 residues followed by a shallow turn and then four more helical residues. The HFP in SDS detergent shows a N-terminal helix followed by a right-angle bend followed by a short C-terminal helix. The beta conformations of FPs have been studied by several biophysical techniques and these studies suggest that these structures correlate with peptide self-association and with interpeptide hydrogen bonding (Gordon et al., 1992; Curtain et al., 1999; Han and Tamm, 2000b). For example, solid-state NMR measurements of membrane-bound HFP are consistent with a mixture of parallel and antiparallel arrangements of beta strands held together by interpeptide hydrogen bonding (Yang and Weliky, 2003).

Another topic of structural and functional interest has been the angle and depth of FP insertion in detergent and in membranes. Most of these insertion studies have focused on the helical forms of FPs. For example, it appears that residues 4–13 of detergent-bound helical HFP are deeply inserted in the micelle and the other residues are solvent exposed (Chang and Cheng, 1998). In addition, several infrared (IR) and electron spin resonance (ESR) studies suggest that the N-terminal helices of the HIV and influenza FPs have an oblique angle of insertion with respect to the membrane bilayer normal (Luneberg et al., 1995; Martin et al., 1996; Macosko et al., 1997). There has been some effort to correlate helix insertion angle and depth with fusogenicity but there is some conflict between various studies. For example, two different groups carried out ESR studies to develop a structural model for the observation that IFP is much more fusogenic at acidic pH than at neutral pH. One of the studies showed a pH-dependence of the helix insertion angle while the other did not show this angle change (Macosko et al., 1997; Zhou et al., 2000; Han et al., 2001). In addition, the G1V mutant of IFP is fusion-inactive and an IR study from one group supported a membrane surface orientation for the peptide while a study from another group supported a transmembrane orientation (Epand et al., 2001; Tamm, 2003). It is also noted that there is evidence for both N- and C-terminal membrane insertion of FPs (Bradshaw et al., 2000). Finally, recent computer simulations of a single HFP

in a membrane bilayer support an oblique N-terminal insertion of wild-type HFP but there is significant disagreement among different simulations about the wild-type HFP insertion depth and about insertion angle and depth for mutant HFPs (Kamath and Wong, 2002; Maddox and Longo, 2002; Wong, 2003).

In the present paper, we investigate application of solid-state NMR for the determination of HFP and IFP orientational distributions in membranes. The membranes are sandwiched between stacked glass plates, and with appropriate hydration, the membranes form planar bilayers whose normal is parallel to the glass plate normal (Marassi et al., 1997). In a typical configuration, the stacked plates are placed in a rectangular coil in the NMR spectrometer so that the glass plate normal is parallel to the applied magnetic field direction. Because of the alignment of the membranes and the magnetic field direction, measurements of anisotropic NMR chemical shifts and dipolar couplings for the peptide can provide information about the peptide orientation relative to the membrane (Ketchem et al., 1993; Opella et al., 1999; Mascioni et al., 2002; Wildman et al., 2003).

In our study, FP orientations are probed with measurements of ^{15}N anisotropic chemical shift distributions at specifically labeled sites in the FP backbone. We seek to address the general questions of whether the approach will be feasible and useful for HIV and influenza FPs and whether any preferred FP orientation can be detected by the approach. We chose ^{15}N labeling for two main reasons: (1) there is an extensive literature of application of ^{15}N NMR for determination of peptide orientation in these types of samples (Ketchem et al., 1993; Bechinger et al., 1993; Yamaguchi et al., 2002; Wildman et al., 2003); and (2) spectral interpretation is aided by the small magnitude of the natural abundance ^{15}N signal relative to the ^{15}N signal of the labeled site. Selective ^{13}C carbonyl labeling is another possibility and one which we initially investigated (Smith et al., 1994). It turned out not to be fruitful because: (1) there was a large natural abundance signal from the lipid carbonyls; and (2) the spectra were low signal-to-noise because of poor cross-polarization for peptide carbonyls at 25–35 °C. We also note that ^{19}F NMR has been applied to determine peptide orientation in glass plate-oriented membrane samples and in particular to a peptide with the sequence of an internal domain of the bindin protein from sea urchin (Afonin et al., 2004). Bindin catalyzes fusion between the membranes of sperm and egg cells during fertilization and the derived peptide also induces intervesicle lipid mixing. ^{19}F NMR has the advantage of high sensitivity but ^{19}F labels must be incorporated into the peptide using non-native amino acids (Afonin et al., 2003).

2. Experimental procedures

2.1. Materials

Rink amide resin was purchased from Advanced Chemtech (Louisville, KY), and 9-fluorenylmethoxycarbonyl (FMOC)-amino acids were obtained from Peptides International (Louisville, KY). Isotopically labeled amino acids were purchased from either Cambridge (Andover, MA) or Icon (Summit, NJ) and were FMOC-protected using literature procedures. 1-Palmitoyl-2-oleoyl-sn-glycero-3-phosphocholine (POPC), 1-palmitoyl-2-oleoyl-sn-glycero-3-phosphoethanolamine (POPE), 1-palmitoyl-2-oleoyl-sn-glycero-3-[phospho-L-serine] (POPS), phosphatidylinositol (PI), sphingomyelin, and 1-palmitoyl-2-oleoyl-sn-glycero-3-[phospho-rac-(1-glycerol)] (POPG) were purchased from Avanti Polar Lipids Inc. (Alabaster, AL).

2.2. Peptides

All HIV peptides were synthesized with a consensus sequence of the 23 N-terminal residues of the LAV_{1a} strain of the HIV-1 gp41 envelope protein followed by additional lysines for improved solubility (Han and Tamm, 2000a). In one construct, a tryptophan was added as a 280 nm chromophore. Peptide constructs are denoted as HFP1 (AVGIGALFLGFLGAAGSTMGARSKKK) and HFP2 (AVGIGALFLGFLGAAGSTMGARSKKKW). Similarly, influenza peptides were synthesized with the 20 N-terminal residues of the HA2 domain of the influenza hemagglutinin fusion protein followed by a glycine/lysine/tryptophan sequence for improved solubility and additional 280 nm chromophores. Peptides are denoted as IFP1 (GLFGAIAGFIENGWEGMIDGGKKK), IFP2 (GLFGAIAGFIENGWEGMIDGGGKKKK), and IFP3 (GLFGAIAGFIENGWEGMIDGGGKKKKWKWK). The peptides were synthesized as their C-terminal amides using

a peptide synthesizer (ABI 431A, Foster City, CA) equipped for FMOC chemistry and then purified by reversed-phase HPLC. Each peptide was labeled with a single backbone ^{13}C carbonyl and/or a single ^{15}N backbone label. For example, HFP2-F8CL9N had a ^{13}C backbone carbonyl label at Phe-8 and a ^{15}N label at Leu-9 and HFP1-L12N had a ^{15}N label at Leu-12.

2.3. Preparation of samples for magic angle spinning (MAS) solid-state NMR

Samples were prepared as previously described (Yang et al., 2001a, 2002). The buffers for the HFP and IFP samples were 5 mM pH 7.0 HEPES and 10 mM pH 5.0 acetate, respectively, which reflect the approximate fusion pHs for the HIV and influenza viruses. Detergent samples were prepared by dissolving lyophilized FP in ∼200 mM DPC solution with final FP concentration of ∼2 mM. For membrane-associated samples, two different membrane compositions were used: (1) 'LM3' had POPC, POPE, POPS, sphingomyelin, PI, and cholesterol in a 10:5:2:2:1:10 mol ratio; and (2) 'PC/PG' had POPC and POPG in a 4:1 mol ratio. PC/PG has been used by other investigators while the LM3 composition reflects the approximate lipid headgroup and cholesterol content of membranes of host cells of the HIV virus and the influenza virus (Milo et al., 1984; Worman et al., 1986; Aloia et al., 1993; Macosko et al., 1997; Han et al., 2001). In the sample preparation protocol, a ∼30 mL FP solution was prepared which contained ∼0.4 μmol FP. FP concentrations were quantitated using either 280 nm absorbance or a bicinchoninic (BCA) assay. Analytical ultracentrifugation data were consistent with predominantly monomeric FP in these solutions (Yang et al., 2004). A ∼5 mL solution was then prepared which contained extruded 150 nm diameter large unilamellar vesicles (LUVs). The LM3 sample preparation used 40 μmol total lipid and 20 μmol cholesterol and the PC/PG sample preparation used 50 μmol total lipid. The FP and LUV solutions were mixed and kept at room temperature overnight. The mixed solution was then ultracentrifuged at ∼100 000 × g for ∼5 h to pellet the LUVs and associated bound FP. Nearly all FP binds to LUVs under these conditions, and unbound FP does not pellet. The total pellet volume was ∼200 μL.

A portion of the FP/LUV pellet formed after ultracentrifugation was transferred by spatula to a MAS NMR rotor. The rotor was sealed with a vespel end cap which had been pre-cooled in liquid nitrogen prior to insertion into the rotor. At liquid nitrogen temperature, the cap fit snugly in the rotor. When the cap warmed up, it formed a tight seal with the rotor which minimized dehydration of the sample.

2.4. Preparation of oriented samples for solid-state NMR

A typical PC/PG sample contained ∼100 μmol total lipid and a typical LM3 sample contained ∼60 μmol total lipid and ∼30 μmol cholesterol. Lipid and cholesterol were dissolved together in chloroform. The chloroform was removed under a stream of nitrogen followed by overnight vacuum pumping. Lipid dispersions were formed by addition of ∼2 mL water followed by homogenization with 10 freeze-thaw cycles. FP (1–2 μmol) was dissolved in ∼2 mL water and then added to the dispersions. The 4 mL mixture was vortexed and then pipetted onto ∼70 glass plates of 6 mm × 13 mm × 0.06 mm dimension (Marienfeld, Lauda-Koenigshofen, Germany). Each plate received a ∼40 μL aliquot of FP/lipid dispersion. Over the course of 1–2 days, bulk water evaporated from the plates. The plates were then stacked inside a rectangular glass tube and the tube was placed in a bottle containing saturated ammonium phosphate solution. The bottle was sealed and placed for several days in a 35 °C incubator to facilitate vapor phase hydration of the membranes. The bottle was then opened and the tube was removed. A specially machined Kel-F plug was inserted into the open end of the tube and then sealed using epoxy. The most reliable sealing results were obtained with 'Extra Setting Time Epoxy Adhesive' from Pacer Technology/Super Glue Corporation (Rancho Cucamonga, CA). In the samples, the NMR spectra of the lipids and FP did not change over the course of at least one month which suggests that their orientational distributions are also constant over this period.

2.5. MAS NMR spectroscopy

The NMR spectra were taken on a 9.4 T spectrometer (Varian Infinity Plus, Palo Alto, CA) using a triple resonance $^{1}H/^{13}C/^{15}N$ MAS probe designed for a 6 mm diameter rotor with 160 μL sample volume. The ^{13}C transmitter was set to ∼155 ppm and the ^{15}N

transmitter was set to ∼120 ppm. ^{13}C chemical shift referencing was done with the methylene resonance of solid adamantane at 40.5 ppm and ^{15}N referencing was done with solid $(NH_4)_2SO_4$ at 27 ppm. The ^{13}C referencing correlates with that used in NMR of soluble proteins (Morcombe and Zilm, 2003). The MAS frequency was 8000 ± 2 Hz and the sample temperatures were between −50 and −80 °C. Previous MAS NMR measurements on membrane-bound FP samples have shown a three-fold improvement in ^{13}C sensitivity at −50 °C relative to room temperature and have also shown that the FP chemical shifts and presumably the FP structure are very similar at the two temperatures (Bodner et al., 2004).

Generation of ^{13}C transverse magnetization with 1–2 ms of ^{1}H–^{13}C cross-polarization at ∼50 kHz Rabi frequency was followed by a 1 ms (eight rotor cycles) ^{13}C–^{15}N REDOR dephasing period and then ^{13}C detection. The REDOR period was used to filter out natural abundance ^{13}C signals from lipid and FP and the resulting spectra were dominated by the signal from the ^{13}C carbonyl label, directly bonded to the ^{15}N amide label (Gullion and Schaefer, 1989; Yang et al., 2002). Filtering was achieved by obtaining 'S_0' and 'S_1' data which were predominantly composed of the total ^{13}C and natural abundance ^{13}C signals, respectively, and by processing the $S_0 - S_1$ difference. The REDOR period for the S_1 data had ^{15}N π pulses at the middle and end of every rotor cycle except for the fourth and eighth cycles while the REDOR period for the S_0 data did not have these pulses. Both the S_0 and S_1 REDOR periods had a ∼50 kHz ^{13}C refocusing π pulse at the end of the fourth rotor cycle. Two-pulse phase modulation ^{1}H decoupling at ∼70 kHz was applied during dephasing and detection (Bennett et al., 1995). The recycle delays were ∼2 s and individual S_0 and S_1 free-induction decays (FIDs) were acquired alternately to obtain optimal compensation of spectrometer instabilities. The S_0–S_1 signal was processed with 50 Hz Gaussian line broadening, Fourier transform, and baseline correction.

2.6. Oriented sample NMR spectroscopy

The NMR spectra of oriented glass plate samples were taken on a 9.4 T spectrometer (Varian Infinity Plus, Palo Alto, CA) using a double resonance ^{1}H/X probe which was designed for static samples and which contained a square coil with 10 mm × 10 mm cross section and 10 mm length. The X channel was tuned to either ^{31}P (referenced to liquid triphenylphosphite at 130 ppm) or to ^{15}N (referenced to solid $(NH_4)_2SO_4$ at 27 ppm). The sample temperature was ∼35 °C. ^{31}P spectra were obtained with a Bloch decay and a ^{31}P $\pi/2$ pulse of ∼5 μs duration, ^{1}H decoupling of ∼30 kHz, and a recycle delay of ∼3 s. ^{15}N NMR spectra were obtained with ∼2 ms of cross-polarization at ∼25 kHz, ^{1}H decoupling of ∼30 kHz, and a recycle delay of ∼1 s. The strength of ^{1}H decoupling was limited by probe arcing. A static ^{15}N spectrum was also obtained for an ultracentrifuged IFP/LUV dispersion made in a manner similar to that of the MAS samples. The dispersion was contained in a 5 mm diameter glass tube and the square coil in the NMR probe was replaced by a 5 mm diameter round coil. The NMR parameters were comparable to those used for the glass plate samples.

3. Results and discussion

3.1. MAS NMR spectra

Fig. 1 displays ^{13}C MAS NMR spectra of (a–c) IFP and (d–f) HFP in different detergent and membrane environments. Because of the REDOR filter, natural abundance ^{13}C signals are attenuated and the spectra are dominated by signals from the Leu-2 and Phe-8 carbonyls of IFP and HFP, respectively. For both FPs, the peak carbonyl chemical shifts are significantly higher in detergent than in LM3 membranes. For IFP in PC/PG membranes, the peak Leu-2 shift is close to that of IFP in detergent, while for HFP in PC/PG membranes, there are two peak Phe-8 shifts, one of which is close to that of HFP in detergent and one of which is close to that of HFP in LM3 membranes.

Both solid-state and liquid-state NMR studies of peptides and proteins have shown that backbone carbonyl chemical shifts are diagnostic of local conformation, with higher shifts in helical conformation and lower shifts in beta strand conformation (Saito, 1986; Zhang et al., 2003). Comparison of the experimental Leu-2 and Phe-8 peak shifts with the shifts characteristic of these residues in different conformations suggests: (1) the Leu-2 local conformation of IFP in detergent and in PC/PG is predominantly helical; (2) the Leu-2 local conformation of IFP in LM3 is predominantly beta strand; and (3) the Phe-8 local conformation

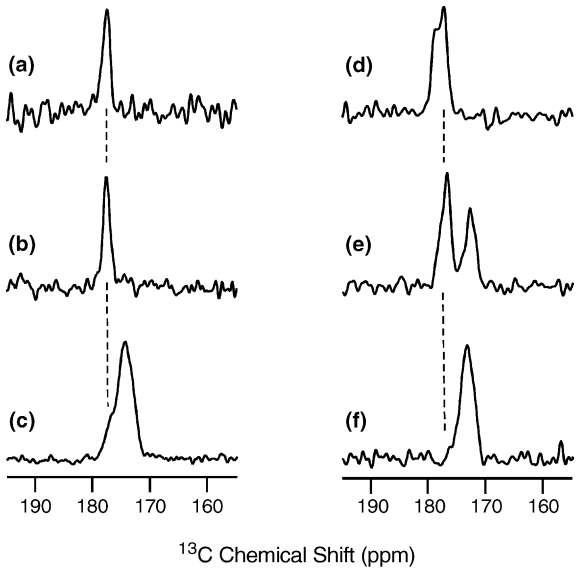

Fig. 1. ^{13}C solid-state MAS NMR spectra of membrane-associated FPs. The samples contained: (a) IFP1-L2CF3N and DPC detergent; (b) IFP3-L2CF3N and PC/PG; (c) IFP3-L2CF3N and LM3; (d) HFP1-F8CL9N and DPC detergent; (e) HFP2-F8CL9N and PC/PG; and (f) HFP2-F8CL9N and LM3. Because of the REDOR filter, the spectra are dominated by the labeled carbonyls. The dashed lines indicate the peak carbonyl chemical shifts for the FPs in DPC detergent. The higher shift for IFP in (a) DPC and (b) PC/PG suggests that Leu-2 has a helical conformation in these environments while the lower shift in (c) LM3 is indicative of beta strand structure. The higher Phe-8 shift of HFP in (d) DPC is characteristic of helical structure, the lower shift in (f) LM3 is characteristic of beta strand structure, and the presence of higher and lower shift components in (e) PC/PG indicates populations of both helical and beta strand structures. Each detergent sample contained ∼2 mM FP and ∼200 mM detergent and each membrane sample contained ∼0.4 μmol FP and 40–50 μmol total lipid. Data were acquired using cross-polarization, 8 kHz MAS frequency, and temperatures of −80 °C for spectra (a and d) and −50 °C for spectra (b, c, e, and f). Each spectrum was processed with 50 Hz Gaussian line broadening and polynomial baseline correction. The total ($S_0 + S_1$) numbers of transients acquired for each spectrum were: (a) 49 530, (b) 29 952, (c) 184 320, (d) 132 524, (e) 140 000, and (f) 186 560.

in HFP is predominantly helical in detergent, predominantly beta strand in LM3, and a mixture of helical and beta strand in PC/PG. For example, the Leu-2 peak shift of IFP in DPC and PC/PG is 177.7 ppm and is more consistent with the 178.5 ± 1.3 ppm shift range of Leu carbonyls in helices than the 175.7 ± 1.5 ppm shift range of Leu carbonyls in beta strands (Zhang et al., 2003). In some contrast, the 174.5 ppm Leu-2 shift of IFP in LM3 is more consistent with beta strand structure. Although the large difference between the two IFP Leu-2 carbonyl shifts strongly indicates that they correspond to different conformations, there is some ambiguity in the conformational assignments based on characteristic chemical shift ranges. One problem is overlap between the 176.9 ± 1.7 ppm shift range of Leu carbonyls in 'coil' conformations (i.e., non-helix, and non-beta strand) and the shift ranges of helix and beta strand conformations. However, for IFP in DPC and PC/PG, the correlation of the Leu-2 shift with helical structure is supported by a significant body of data from our and other groups (Macosko et al., 1997; Han and Tamm, 2000a; Han et al., 2001). The biophysical techniques used in these studies include IR, circular dichroism, ESR, and liquid-state NMR spectroscopies, as well as solid-state NMR internuclear distance measurements (P.D. Parkanzky and D.P. Weliky, unpublished data). Although there have not been other structural studies of IFP in LM3, there is one combined IR and membrane binding study of IFP in PC/PG in which beta strand structure was detected at high peptide:lipid ratio and high salt concentration (Han and Tamm, 2000b). In addition, analysis of the binding data was consistent with a free energy change of −1.9 kcal/mol for peptide self-association in membranes.

For HFP in DPC, the Phe-8 peak shift of 177.4 ppm is consistent with the 177.1 ± 1.4 ppm shift range of Phe in helices. In some contrast, the 173.4 ppm Phe-8 shift of HFP in LM3 correlates with the 174.3 ± 1.6 ppm shift range of Phe in beta strands. For HFP in PC/PG, the 177.0 ppm peak likely corresponds to a population of helical peptide and the 172.9 ppm peak likely corresponds to a different population of beta strand peptide. The helical structure interpretation of the solid-state NMR data in DPC is consistent with a solution NMR study which showed an overall helical conformation of HFP in detergent (Chang et al., 1997). The beta strand interpretation of the solid-state NMR data in LM3 is consistent with previous measurements of chemical shifts of other carbonyl, Cα, and Cβ nuclei in LM3-bound HFP and with analysis of spectral intensities in 2D MAS exchange experiments on this system (Yang et al., 2001a; Bodner et al., 2004). In addition, solid-state NMR internuclear distance measurements have demonstrated that the HFP beta strand structure in LM3 is oligomeric and has interpeptide hydrogen bonds (Yang and Weliky, 2003).

In summary, the ^{13}C MAS NMR measurements of this paper show that both IFP and HFP exhibit structural plasticity and that the distribution of conformations in membranes depends in part on the detergent and membrane composition. Although, we do not yet have a clear understanding of the switch from helical conformation in PC/PG to beta strand in LM3, other solid-state NMR spectra suggest that the presence of cholesterol in LM3 and its absence in PC/PG plays some role in the conformational change (Yang et al., 2002).

3.2. Oriented sample NMR spectra

In order to obtain meaningful information from NMR spectra of glass plate samples containing FPs and membranes, the membrane bilayer and glass plate normals should be collinear. As displayed in Fig. 2, ^{31}P NMR spectra can provide experimental evidence for collinearity, including: (1) narrow linewidth; and (2) downfield and upfield dependence of the peak shifts on respective parallel and perpendicular orientations

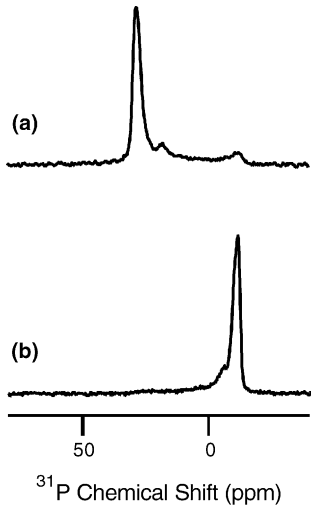

Fig. 2. ^{31}P solid-state NMR spectra of a glass plate sample containing IFP2-F3N and PC/PG at peptide:lipid ∼0.02. The glass plate normal was either (a) parallel or (b) perpendicular to the external magnetic field. The chemical shift of the dominant peak varies significantly as a function of glass plate orientation and is consistent with oriented bilayers whose normal is parallel to the glass plate normal. Data were acquired using a Bloch decay and 35 °C sample temperature. Each spectrum represents the sum of 16 transients and was processed with 50 Hz line broadening.

of the glass plate normal relative to the magnetic field direction (Smith et al., 1992; Mascioni et al., 2002). ^{31}P spectra of all of our glass plate samples were consistent with predominant collinearity of the bilayer and glass plate normals. As evidenced by the small upfield component in Fig. 2(a), most samples also contained a minor population of unoriented bilayers, but the much larger population of oriented bilayers was adequate to proceed with ^{15}N NMR studies of FP orientation relative to the bilayers. We do note that both the population of unoriented bilayers and the ^{31}P line-width of the oriented component were generally larger in samples which contained FP relative to samples which did not contain FP (Yang et al., 2001b). These data suggest that membranes do not orient as well in the presence of FP and this observation may be related to FP-induced membrane curvature and to FP catalysis of membrane fusion (Epand, 2003).

As displayed in Fig. 1, the FP conformational distributions are different in PC/PG and LM3 membranes and we made glass plate samples with both membrane compositions. Fig. 3(a and b) shows ^{15}N NMR spectra from samples which contained HFP1-L12N and LM3 and for which HFP likely has a beta strand conformation (Fig. 1f). The glass plate normal was oriented either (a) parallel or (b) perpendicular to the magnetic field direction. The line-shapes are much broader than the 10–20 ppm line-widths typically seen for samples in which the peptide is well-aligned in the membrane. The spectra also have greater intensity upfield and lower intensity downfield which is qualitatively characteristic of a random ‘powder pattern’ distribution of peptide molecules (Lazo et al., 1995). However, there are differences between the shapes of the two spectra in Fig. 3(a and b) and these differences would not be expected for completely randomly oriented peptide. Overall, the data suggest that the distribution of peptide orientations in the membrane has some breadth but is not completely random. More detailed understanding of the orientational distribution should be based on line-shape simulations for different orientational models.

Fig. 3(c and d) shows ^{15}N NMR spectra from a sample which contain HFP1-V2CA6N and PC/PG and for which there are likely populations of both helical and beta strand conformations (Fig. 1e). The V2C label has no effect on the ^{15}N spectra and the glass plate normal was oriented either (c) parallel or (d) perpendicular to the magnetic field direction. These spectra appear to

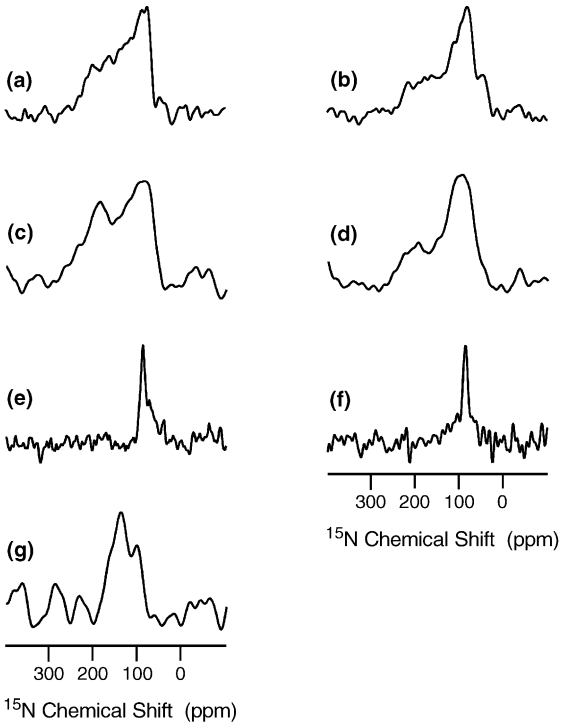

Fig. 3. ^{15}N static solid-state NMR spectra of membrane-associated FPs. Spectra (a and b) were obtained with samples containing HFP1-L12N and LM3; spectra (c and d) were obtained with a sample containing HFP1-V2CA6N and PC/PG; spectra (e and g) were obtained with samples containing IFP2-A7N and PC/PG; and spectrum (f) was obtained with a sample containing IFP2-F3N and PC/PG. The FP:lipid ratio in all samples was ∼0.02. Spectra (a–f) were obtained with glass plate samples and the glass plate normal was parallel to the magnetic field for spectra (a, c, e, and f) and perpendicular to the field for spectra (b and d). The sample for spectrum (g) was a IFP/LUV dispersion. Data were acquired using cross-polarization and 35 °C sample temperature. Spectra (a and b) were processed with 400 Hz line broadening, spectra (c, d, and g) were processed with 800 Hz line broadening, and spectra (e and f) were processed with 200 Hz line broadening. The total numbers of transients acquired for each spectrum were: (a) 87 498, (b) 100 369, (c) 80 000, (d) 80 000, (e) 200 000, (f) 200 000, and (g) 778 608.

have a broad component and also an additional peak at ∼190 ppm in the parallel orientation. We tentatively assign this peak to helical peptide and the downfield value of its anisotropic shift in the parallel orientation is consistent with an oriented helix whose axis is closer to the bilayer normal than to the bilayer surface (Marassi et al., 1997). We note that another group has also studied an ^{15}N labeled HFP in a PC/PG glass plate sample and obtained a downfield anisotropic shift for Ala-6 close to our observed 190 ppm value (F.M. Marassi, personal communication).

Although the HFP spectra in PC/PG were complicated by the presence of two HFP conformations, they pointed us towards making samples with IFP in PC/PG because IFP is predominantly helical in this composition (Fig. 1b). Spectra from two such samples are displayed in Fig. 3(e and f) and contained either IFP2-A7N or IFP2-F3N peptides, respectively. Both spectra were obtained for a parallel orientation of the plate normal and magnetic field direction. Each spectrum is composed of a peak with ∼10 ppm full-width at half-maximum line-width. The sharpness of the peaks suggests that helical IFP is well-oriented and the upfield anisotropic shifts of the peaks are consistent with a helix axis orientation which is closer to the surface of the bilayer than to the bilayer normal (Marassi et al., 1997). When the glass plate normal was oriented perpendicular to the magnetic field direction, low signal-to-noise spectra were obtained and did not have the sharp downfield feature. Similar observations of strong signals in the parallel orientation and no signal in the perpendicular orientation have been reported by the Ramamoorthy group for the helical antimicrobial peptide LL-37 in stacked glass plate samples (Wildman et al., 2003). As described in the Ramamoorthy paper, one explanation for this observation is that the spectrum is broader in the perpendicular plate orientation relative to the parallel orientation. LL-37 is similar to IFP in having its helix axis approximately parallel to the membrane surface. For an ensemble of either IFP or LL-37 peptides, individual molecules may differ in their azimuthal orientation relative to the membrane bilayer normal. The different azimuthal orientations are related by rotation about the bilayer normal direction. For the parallel plate orientation, the membrane normal and magnetic field are collinear, and the different azimuthal orientations all result in the same anisotropic ^{15}N shift and a sharp spectrum. In the perpendicular plate orientation, different azimuthal orientations can have different ^{15}N shifts with a resulting broader spectrum (Smith et al., 1994).

In addition to the static broadening described in the above paragraph, slow rotational motion of peptides about the bilayer normal could specifically attenuate the spectrum in the perpendicular plate orientation through introduction of additional spectral broadening and interference with cross-polarization. With this in

mind, peptide motion in our samples was considered through qualitative analysis of the spectra in Fig. 3. For example, the spectral breadths in Fig. 3(a and b) are close to what is observed in lyophilized peptides, and suggest that beta strand FPs do not undergo large motion (Lazo et al., 1995). To gain insight into motion of helical FPs, an unoriented dispersion sample without glass plates was prepared which contained ultracentrifuged PC/PG LUVs and associated IFP2-A7N peptide. The spectrum of this sample is displayed in Fig. 3(g) and has low signal-to-noise, perhaps due to inefficient cross-polarization arising from peptide motion. The spectrum appears narrower than the spectra in Fig. 3(a and b) which is also indicative of motion of helical IFP. However, in this sample, a possible confounding factor is the motion of the vesicles in the dispersion. To address this problem, we plan to study a sample where IFP is added to a PC/PG dispersion which has not been extruded into vesicles.

3.3. Comparison with other studies and future experiments

The principle solid-state NMR results of this paper are: (1) FP conformational distributions depend strongly on the lipid headgroup and cholesterol composition of the associated membrane; (2) there appears to be breadth in the orientational distribution of beta strand HFPs in membranes; (3) helical FPs appear to orient well in membranes; and (4) the helix axes of HFP and IFP appear to be different with the HFP axis closer to the membrane bilayer normal and the IFP axis closer to the membrane surface. Overall, our results are consistent with at least some previous studies and suggest several future experiments. For example, conformational plasticity of FPs has been reported in earlier studies using techniques other than solid-state NMR (Durell et al., 1997; Epand, 2003). However, to our knowledge, these studies did not carefully investigate the dependence of conformation on lipid and cholesterol composition, as is reported in this paper. Using our results, it should be possible to study the dependence of fusogenicity on conformation by carrying out comparative functional fusion assays using the same FP and LUVs with either PC/PG or LM3 composition. Preliminary data from our group are consistent with significant fusion activity for LUVs of either composition and suggest that a FP can be fusogenic and adopt either helical or beta strand conformation in its final membrane-associated form.

The breadth of orientational preference for HFP beta strands and the orientations of the HFP and IFP helices derived from our solid-state NMR experiments can be compared with some of the previous IR, ESR, and computational studies on these systems (Martin et al., 1993, 1996; Luneberg et al., 1995; Macosko et al., 1997; Han and Tamm, 2000a; Han et al., 2001; Kamath and Wong, 2002; Maddox and Longo, 2002). There is qualititative agreement with the results of some of these studies. For example, oriented HFP beta strands were not detected in IR experiments (Martin et al., 1993). In addition, an ESR study yielded a $\sim 65^{\circ}$ angle between the IFP helix axis and the bilayer normal (Macosko et al., 1997) while a computational study yielded a $\sim 35^{o}$ angle between the HFP helix axis and the bilayer normal (Maddox and Longo, 2002). These results are consistent with our model of helix axis orientations based on anisotropic ^{15}N shifts for IFP and HFP in PC/PG.

One promising aspect of our study is that the helical form of IFP is highly oriented in glass plate samples so that future studies should be able to precisely define helix orientation(s) using additional measurements of anisotropic ^{15}N chemical shifts and ^{1}H–^{15}N dipolar couplings, and perhaps also using 2D PISEMA correlation between these shifts and couplings (Ketchem et al., 1993; Wildman et al., 2003; Opella and Marassi, 2004; Ramamoorthy et al., 2004). Similar determinations of helix orientations in mutant peptides should be able to distinguish between different literature models which correlate IFP helix orientation with fusogenicity (Epand et al., 2001; Tamm, 2003). A current project in our laboratory is to determine whether there is a change in the IFP helix orientation as a function of pH which might then be correlated with the observed increased IFP fusogenicity at lower pH. This work might help to resolve the disagreement between different ESR studies on this question. (Zhou et al., 2000; Han et al., 2001).

The data presented in this paper suggest that solid-state NMR determination of HFP orientation in either its helical or beta strand conformations may be problematic because: (1) the beta strands do not appear to be strongly oriented in LM3; and (2) there is a mixture of unoriented beta strands and possibly oriented helices in PC/PG. However, it may be possible to address these problems by using C-terminal cross-linked HFPs (Yang et al., 2003). These cross-linked peptides were

synthesized to mimic the expected oligomeric topology of HFPs as part of the gp41 protein. Both the gp41 and the hemagglutinin proteins form trimers and structural studies suggest that the protein regions C-terminal of the three FPs are close together in space (Eckert and Kim, 2001). Work from our group has shown that dimeric and trimeric cross-linked HFPs (denoted as HFPdm and HFPtr) induce both more fusion and a much faster rate of fusion than the non-cross-linked HFP (denoted as HFPmn) which indicates that the oligomeric FP topology is functionally important. In addition, solid-state NMR measurements of ^{13}C chemical shifts and internuclear distances have shown that the HFPtr is predominantly helical in PC/PG, which is quite different from the mixed conformations observed for HFPmn in PC/PG. Because of the conformational homogeneity of HFPtr, NMR studies of glass plate samples containing ^{15}N-labeled HFPtr and PC/PG will likely provide clear information about helix orientation. In LM3, HFPtr has been shown to have beta strand conformation and experimental data and biophysical reasoning suggest that the HFPtr strands may be better oriented than those of HFPmn. It was previously shown by solid-state NMR experiments that beta strand HFPmn in LM3 contains a mixture of parallel and antiparallel strand arrangements and this mixed structure could result in a broad distribution of strand orientations relative to the membrane (Yang and Weliky, 2003). In some contrast, the C-terminal cross-linking of HFPtr may favor formation of a more homogeneous parallel strand arrangement with a resulting more uniform strand orientation.

In summary, ^{15}N solid-state NMR of influenza and HIV FPs in glass plate samples appears to be a promising approach for obtaining peptide orientational information and for understanding fusogenic function.

Acknowledgements

We acknowledge financial support from NIH grant AI47153, the Camille and Henry Dreyfus Foundation, the Michigan State Intramural Research Grants Program, and the Michigan State Center for Biological Modeling. The NMR instruments were purchased with support from NSF grant 9977650. We also acknowledge assistance from Jun Yang in peptide synthesis and in acquisition of some of the NMR spectra.

References

Afonin, S., Dur, U.H.N., Glaser, R.W., Ulrich, A.S., 2004. 'Boomerang'-like insertion of a fusogenic peptide in a lipid membrane revealed by solid-state ^{19}F NMR. Magn. Reson. Chem. 42, 195–203.

Afonin, S., Glaser, R.W., Berditchevskaia, M., Wadhwani, P., Guhrs, K.H., Mollmann, U., Perner, A., Ulrich, A.S., 2003. 4-Fluorophenylglycine as a label for ^{19}F NMR structure analysis of membrane-associated peptides. Chembiochem 4, 1151–1163.

Aloia, R.C., Tian, H., Jensen, F.C., 1993. Lipid composition and fluidity of the human immunodeficiency virus envelope and host cell plasma membranes. Proc. Natl. Acad. Sci. USA 90, 5181–5185.

Bechinger, B., Zasloff, M., Opella, S.J., 1993. Structure and orientation of the antibiotic peptide magainin in membranes by solid-state nuclear-magnetic-resonance spectroscopy. Protein Sci. 2, 2077–2084.

Bennett, A.E., Rienstra, C.M., Auger, M., Lakshmi, K.V., Griffin, R.G., 1995. Heteronuclear decoupling in rotating solids. J. Chem. Phys. 103, 6951–6958.

Blumenthal, R., Clague, M.J., Durell, S.R., Epand, R.M., 2003. Membrane fusion. Chem. Rev. 103, 53–69.

Bodner, M.L., Gabrys, C.M., Parkanzky, P.D., Yang, J., Duskin, C.A., Weliky, D.P., 2004. Temperature dependence and resonance assignment of ^{13}C NMR spectra of selectively and uniformly labeled fusion peptides associated with membranes. Magn. Reson. Chem. 42, 187–194.

Bradshaw, J.P., Darkes, M.J., Harroun, T.A., Katsaras, J., Epand, R.M., 2000. Oblique membrane insertion of viral fusion peptide probed by neutron diffraction. Biochemistry 39, 6581–6585.

Bullough, P.A., Hughson, F.M., Skehel, J.J., Wiley, D.C, 1994. Structure of influenza haemagglutinin at the pH of membrane fusion. Nature 371, 37–43.

Carr, C.M., Kim, P.S., 1993. A spring-loaded mechanism for the conformational change of influenza hemagglutinin. Cell 73, 823–832.

Chang, D.K., Cheng, S.F., 1998. Determination of the equilibrium micelle-inserting position of the fusion peptide of gp41 of human immunodeficiency virus type 1 at amino acid resolution by exchange broadening of amide proton resonances. J. Biomol. NMR 12, 549–552.

Chang, D.K., Cheng, S.F., Chien, W.J., 1997. The amino-terminal fusion domain peptide of human immunodeficiency virus type 1 gp41 inserts into the sodium dodecyl sulfate micelle primarily as a helix with a conserved glycine at the micelle-water interface. J. Virol. 71, 6593–6602.

Curtain, C., Separovic, F., Nielsen, K., Craik, D., Zhong, Y., Kirkpatrick, A., 1999. The interactions of the N-terminal fusogenic peptide of HIV-1 gp41 with neutral phospholipids. Eur. Biophys. J. 28, 427–436.

Delahunty, M.D., Rhee, I., Freed, E.O., Bonifacino, J.S., 1996. Mutational analysis of the fusion peptide of the human immunodeficiency virus type 1: identification of critical glycine residues. Virology 218, 94–102.

Dubovskii, P.V., Li, H., Takahashi, S., Arseniev, A.S., Akasaka, K., 2000. Structure of an analog of fusion peptide from hemagglutinin. Protein Sci. 9, 786–798.

Durell, S.R., Martin, I., Ruysschaert, J.M., Shai, Y., Blumenthal, R., 1997. What studies of fusion peptides tell us about viral envelope glycoprotein-mediated membrane fusion (review). Mol. Membr. Biol. 14, 97–112.

Durrer, P., Galli, C., Hoenke, S., Corti, C., Gluck, R., Vorherr, T., Brunner, J., 1996. H^+-induced membrane insertion of influenza virus hemagglutinin involves the HA2 amino-terminal fusion peptide but not the coiled coil region. J. Biol. Chem. 271, 13417–13421.

Eckert, D.M., Kim, P.S., 2001. Mechanisms of viral membrane fusion and its inhibition. Annu. Rev. Biochem. 70, 777–810.

Epand, R.M., 2003. Fusion peptides and the mechanism of viral fusion. Biochim. Biophys. Acta-Biomembr. 1614, 116–121.

Epand, R.M., Epand, R.F., Martin, I., Ruysschaert, J.M., 2001. Membrane interactions of mutated forms of the influenza fusion peptide. Biochemistry 40, 8800–8807.

Freed, E.O., Delwart, E.L., Buchschacher Jr., G.L., Panganiban, A.T., 1992. A mutation in the human immunodeficiency virus type 1 transmembrane glycoprotein gp41 dominantly interferes with fusion and infectivity. Proc. Natl. Acad. Sci. USA 89, 70–74.

Gething, M.J., Doms, R.W., York, D., White, J., 1986. Studies on the mechanism of membrane-fusion - site-specific mutagenesis of the hemagglutinin of influenza-virus. J. Cell Biol. 102, 11–23.

Gordon, L.M., Curtain, C.C., Zhong, Y.C., Kirkpatrick, A., Mobley, P.W., Waring, A.J., 1992. The amino-terminal peptide of HIV-1 glycoprotein 41 interacts with human erythrocyte membranes: peptide conformation, orientation and aggregation. Biochim. Biophys. Acta 1139, 257–274.

Gullion, T., Schaefer, J., 1989. Rotational-echo double-resonance NMR. J. Magn. Reson. 81, 196–200.

Han, X., Bushweller, J.H., Cafiso, D.S., Tamm, L.K., 2001. Membrane structure and fusion-triggering conformational change of the fusion domain from influenza hemagglutinin. Nat. Struct. Biol. 8, 715–720.

Han, X., Tamm, L.K., 2000a. A host-guest system to study structure-function relationships of membrane fusion peptides. Proc. Natl. Acad. Sci. USA 97, 13097–13102.

Han, X., Tamm, L.K., 2000b. pH-dependent self-association of influenza hemagglutinin fusion peptides in lipid bilayers. J. Mol. Biol. 304, 953–965.

Hernandez, L.D., Hoffman, L.R., Wolfsberg, T.G., White, J.M., 1996. Virus–cell and cell–cell fusion. Annu. Rev. Cell Dev. Biol. 12, 627–661.

Hsu, C.H., Wu, S.H., Chang, D.K., Chen, C.P., 2002. Structural characterizations of fusion peptide analogs of influenza virus hemagglutinin — implication of the necessity of a helix-hinge-helix motif in fusion activity. J. Biol. Chem. 277, 22725–22733.

Kamath, S., Wong, T.C., 2002. Membrane structure of the human immunodeficiency virus gp41 fusion domain by molecular dynamics simulation. Biophys. J. 83, 135–143.

Ketchem, R.R., Hu, W., Cross, T.A., 1993. High-resolution conformation of gramicidin A in a lipid bilayer by solid-state NMR. Science 261, 1457–1460.

Lazo, N.D., Hu, W., Cross, T.A., 1995. Low-temperature solid-state ^{15}N NMR characterization of polypeptide backbone librations. J. Magn. Reson. Ser. B 107, 43–50.

Luneberg, J., Martin, I., Nussler, F., Ruysschaert, J.M., Herrmann, A., 1995. Structure and topology of the influenza-virus fusion peptide in lipid bilayers. J. Biol. Chem. 270, 27606–27614.

Macosko, J.C., Kim, C.H., Shin, Y.K., 1997. The membrane topology of the fusion peptide region of influenza hemagglutinin determined by spin-labeling EPR. J. Mol. Biol. 267, 1139–1148.

Maddox, M.W., Longo, M.L., 2002. Conformational partitioning of the fusion peptide of HIV-1 gp41 and its structural analogs in bilayer membranes. Biophys. J. 83, 3088–3096.

Marassi, F.M., Ramamoorthy, A., Opella, S.J., 1997. Complete resolution of the solid-state NMR spectrum of a uniformly ^{15}N-labeled membrane protein in phospholipid bilayers. Proc. Natl. Acad. Sci. USA 94, 8551–8556.

Martin, I., Defrise-Quertain, F., Decroly, E., Vandenbranden, M., Brasseur, R., Ruysschaert, J.M., 1993. Orientation and structure of the NH_2-terminal HIV-1 gp41 peptide in fused and aggregated liposomes. Biochim. Biophys. Acta 1145, 124–133.

Martin, I., Schaal, H., Scheid, A., Ruysschaert, J.M., 1996. Lipid membrane fusion induced by the human immunodeficiency virus type 1 gp41 N-terminal extremity is determined by its orientation in the lipid bilayer. J. Virol. 70, 298–304.

Mascioni, A., Karim, C., Zamoon, J., Thomas, D.D., Veglia, G., 2002. Solid-state NMR and rigid body molecular dynamics to determine domain orientations of monomeric phospholamban. J. Am. Chem. Soc. 124, 9392–9393.

Milo, G.E., Ackerman, G.A., Sanders, R.L., 1984. Growth-characteristics, morphology, and phospholipid-composition of human type-II pulmonary alveolar cells grown in a collagen-free microenvironment. In Vitro 20, 899–911.

Morcombe, C.R., Zilm, K.W., 2003. Chemical shift referencing in MAS solid state NMR. J. Magn. Reson. 162, 479–486.

Opella, S.J., Marassi, F.M., 2004. Structure determination of membrane proteins by NMR spectroscopy. Chem. Rev. 104, 3587–3606.

Opella, S.J., Marassi, F.M., Gesell, J.J., Valente, A.P., Kim, Y., Oblatt-Montal, M., Montal, M., 1999. Structures of the M2 channel-lining segments from nicotinic acetylcholine and NMDA receptors by NMR spectroscopy. Nat. Struct. Biol. 6, 374–379.

Pereira, F.B., Goni, F.M., Muga, A., Nieva, J.L., 1997. Permeabilization and fusion of uncharged lipid vesicles induced by the HIV-1 fusion peptide adopting an extended conformation: dose and sequence effects. Biophys. J. 73, 1977–1986.

Pritsker, M., Rucker, J., Hoffman, T.L., Doms, R.W., Shai, Y., 1999. Effect of nonpolar substitutions of the conserved Phe11 in the fusion peptide of HIV-1 gp41 on its function, structure, and organization in membranes. Biochemistry 38, 11359–11371.

Rafalski, M., Lear, J.D., DeGrado, W.F., 1990. Phospholipid interactions of synthetic peptides representing the N- terminus of HIV gp41. Biochemistry 29, 7917–7922.

Ramamoorthy, A., Wei, Y., Lee, D.K., 2004. PISEMA Solid-state NMR Spectroscopy. Elsevier, London.

Saez-Cirion, A., Nieva, J.L., 2002. Conformational transitions of membrane-bound HIV-1 fusion peptide. Biochim. Biophys. Acta-Biomembr. 1564, 57–65.

Saito, H., 1986. Conformation-dependent ^{13}C chemical-shifts — a new means of conformational characterization as obtained by

high-resolution solid-state ^{13}C NMR. Magn. Reson. Chem. 24, 835–852.

Smith, R., Separovic, F., Bennett, F.C., Cornell, B.A., 1992. Melittin-induced changes in lipid multilayers. A solid-state NMR study. Biophys. J. 63, 469–474.

Smith, R., Separovic, F., Milne, T.J., Whittaker, A., Bennett, F.M., Cornell, B.A., Makriyannis, A., 1994. Structure and orientation of the pore-forming peptide, melittin, in lipid bilayers. J. Mol. Biol. 241, 456–466.

Tamm, L.K., 2003. Hypothesis: spring-loaded boomerang mechanism of influenza hemagglutinin-mediated membrane fusion. Biochim. Biophys. Acta-Biomembr. 1614, 14–23.

Wildman, K.A.H., Lee, D.K., Ramamoorthy, A., 2003. Mechanism of lipid bilayer disruption by the human antimicrobial peptide, LL-37. Biochemistry 42, 6545–6558.

Wilson, I.A., Skehel, J.J., Wiley, D.C., 1981. Structure of the haemagglutinin membrane glycoprotein of influenza virus at 3 Å resolution. Nature 289, 366–373.

Wong, T.C., 2003. Membrane structure of the human immunodeficiency virus gp41 fusion peptide by molecular dynamics simulation. II. The glycine mutants. Biochim. Biophys. Acta-Biomembr. 1609, 45–54.

Worman, H.J., Brasitus, T.A., Dudeja, P.K., Fozzard, H.A., Field, M., 1986. Relationship between lipid fluidity and water permeability of bovine tracheal epithelial–cell apical membranes. Biochemistry 25, 1549–1555.

Yamaguchi, S., Hong, T., Waring, A., Lehrer, R.I., Hong, M., 2002. Solid-state NMR investigations of peptide-lipid interaction and orientation of a β-sheet antimicrobial peptide, protegrin. Biochemistry 41, 9852–9862.

Yang, J., Gabrys, C.M., Weliky, D.P., 2001a. Solid-state nuclear magnetic resonance evidence for an extended beta strand conformation of the membrane-bound HIV-1 fusion peptide. Biochemistry 40, 8126–8137.

Yang, J., Parkanzky, P.D., Khunte, B.A., Canlas, C.G., Yang, R., Gabrys, C.M., Weliky, D.P., 2001b. Solid state NMR measurements of conformation and conformational distributions in the membrane-bound HIV-1 fusion peptide. J. Mol. Graphics Modell. 19, 129–135.

Yang, J., Parkanzky, P.D., Bodner, M.L., Duskin, C.G., Weliky, D.P., 2002. Application of REDOR subtraction for filtered MAS observation of labeled backbone carbons of membrane-bound fusion peptides. J. Magn. Reson. 159, 101–110.

Yang, R., Yang, J., Weliky, D.P., 2003. Synthesis, enhanced fusogenicity, and solid state NMR measurements of cross-linked HIV-1 fusion peptides. Biochemistry 42, 3527–3535.

Yang, J., Weliky, D.P., 2003. Solid state nuclear magnetic resonance evidence for parallel and antiparallel strand arrangements in the membrane-associated HIV-1 fusion peptide. Biochemistry 42, 11879–11890.

Yang, J., Prorok, M., Castellino, F.J., Weliky, D.P., 2004. Oligomeric β-structure of the membrane-bound HIV-1 fusion peptide formed from soluble monomers. Biophys. J. 87, 1951–1963.

Zhang, H.Y., Neal, S., Wishart, D.S., 2003. RefDB: A database of uniformly referenced protein chemical shifts. J. Biomol. NMR 25, 173–195.

Zhou, Z., Macosko, J.C., Hughes, D.W., Sayer, B.G., Hawes, J., Epand, R.M., 2000. ^{15}N NMR study of the ionization properties of the influenza virus fusion peptide in zwitterionic phospholipid dispersions. Biophys. J. 78, 2418–2425.